Test Beam 2005

April 25, 2005

Abstract

The performance of LHCb Outer Tracker modules will be presented, as read out with the final front end electronics. An electron beam of 6 GeV was used obtained from the DESYII facility in Hamburg.

Note

Issue	11
Reference	
Created	April 7, 2005
Last Modified	April 25, 2005

Prepared by

NIKHEF, Amsterdam, The Netherlands

Physikalisches Institut, Heidelberg, Germany

Contents

List of Figures

1 Introduction

The purpose of these studies was to test mass production modules of the LHCb Outer Tracker, in combination with final version of frontend electronics, at the beam and measure main parameters of the detector. The chambers were tested in the experimental area 22 of DESY at the DESYII accelerator, with an electron beam of 6 GeV. Some runs have been taken down to 1 GeV.

2 Test setup

The schematic setup layout is shown in Fig.1.

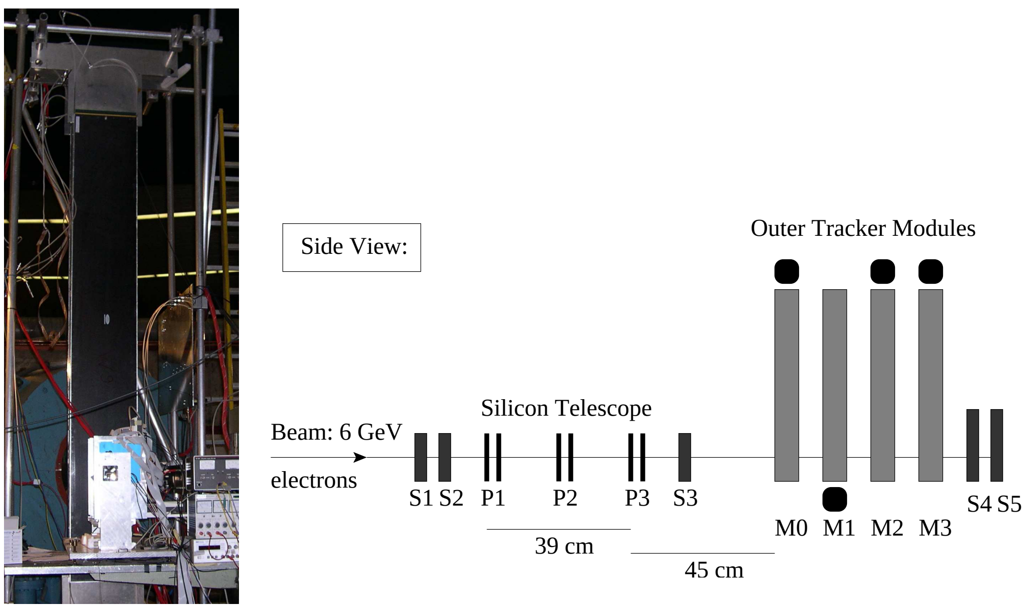

Figure 1: *(a) A photograph (front view) of the OT modules is shown and (b) a schematic picture of the setup is shown.*

The test setup comprised four "short" OT modules, which are 2.25 m long double layer straw chambers. The setup contained a total of eight monolayers, or planes, of straws. [1] The chambers were installed vertically

[1]Throughout this note the modules and planes will be referred to according to their position along the beam starting from 1, *i.e.* modules 1–4 and planes 1–8.

on a moveable platform. The gas mixture used in these tests was 70% Ar and 30% CO_2.

Each chamber was equipped with the standard, final, frontend box. The output signals from each frontend box were transmitted through an optical line to the data acquisition system based on the Texas Instruments TLK2501 receiver and de-serializer chip and ALTERA Stratix FPGA.

In order to have a possibility to independently measure the track parameters, a silicon strip telescope was used. The number of OT modules (4 modules, or 8 monolayers), however, was sufficient to reconstruct tracks using OT data alone. Most results including the silicon tracks will be discussed elsewhere, but in this note some basic quantities of the OT tracks are shown to be consistent with the Si tracks.

The trigger signal, which served also as time reference, was produced by coincidence of two scintillator counters installed downstream of the OT modules.

2.1 Beam

For the OT studies in most cases the beam of maximum possible energy, 6 GeV, was used, in order to minimize multiple scattering in the setup. The OT hit map is shown in Fig.2, for the cases when Si telescope was used (*a*) and not used (*b*). In case of using the Si telescope the beam is rather narrow, allowing us to illuminate only one full straw per OT plane. When only OT modules were used, several (5-7) full straws were iluminated.

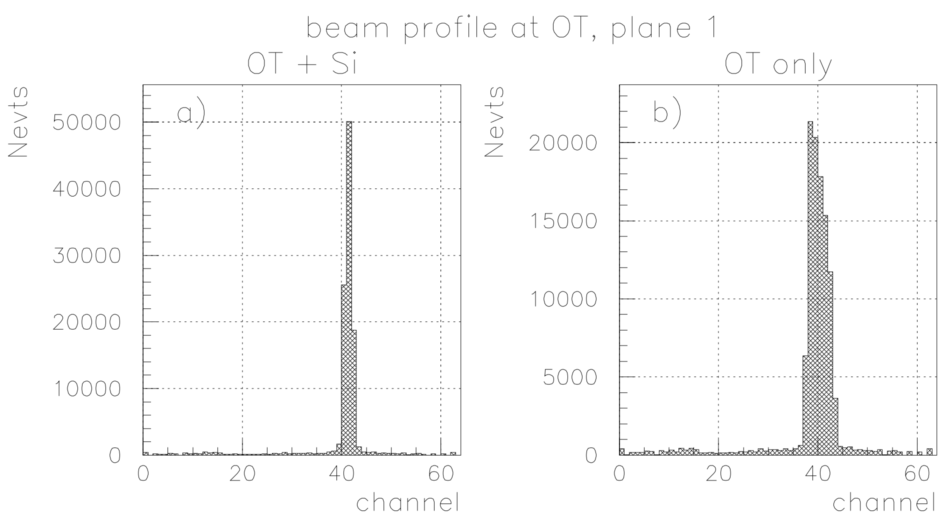

Figure 2: *The OT hit maps for the plane 1 (the upstream plane of the first module), for the cases of working with (a) and without (b) the Si telescope.*

2.2 Trigger timing and OT drift time distribution

In order to measure the OT drift times, the time reference provided by scintillators was used: the arrival time of scintillator signals was also measured by OTIS TDCs and then subtracted from the arrival times of OT signals. The average time of the two scintillators was used as time reference:

$$t_{ref} = \frac{t_{SC1} + t_{SC2}}{2}.$$

The precision of the time reference, evaluated from the distribution of time difference of the two scintillators, was about 0.5 ns, which is negligble compared to the drift time resolution[2].

The raw time distribution of OT signals is shown in Fig.3*a*: it fits well into the 75 ns time window of OTIS. The OT drift time distribution is shown in Fig.3*b*.

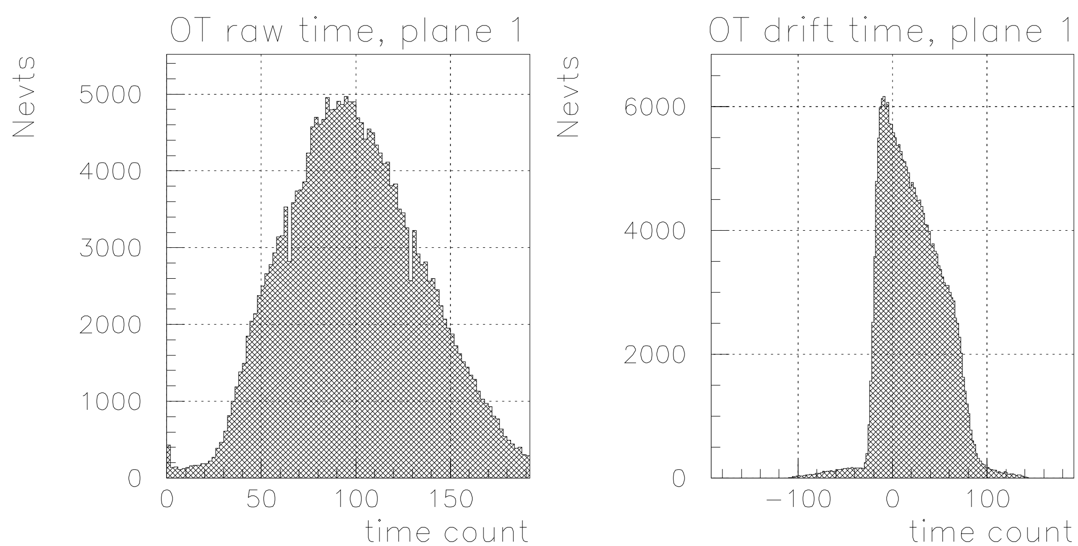

Figure 3: *The arrival time distribution of OT hits (a) and drift time distribution (b), at 1580 V. Note that 64 units correspond to 25 ns.*

[2]% The maximum drift time of approximately 50 ns corresponds to the straw diameter of 2.495 mm, hence a time smearing of 0.5 ns would add a smearing in the position determination of about 25 μm.

3 Analysis

3.1 OT standalone analysis

The setup included a total of eight straw planes, which is sufficient to reliably reconstruct tracks and obtain estimates of the detector characteristics. The analysis was performed in exactly the same way as that for the OT TDR (see [1] and references therein; a comprehensive description of the analysis basics can be found in [2]).

In the OT standalone analysis the following procedure was applied. A hit was used in the track, if the drift time is in agreement with the track prediction within 6σ. Only those tracks were kept which had at least 4 hits and a track length along the beam direction of at least 150 mm.

The event was used for subsequent analysis if it had only one track; this requirement rejected 5–7% of the events.

3.2 Alignment of OT modules in z

Several runs were taken in which both the Si and the OT were read out, with all the OT planes being at nominal settings. This gives the possibility to compare the two independent track reconstruction algorithms with the Si and the OT. In addition, this allows for a relative alignment of the Si and OT systems.

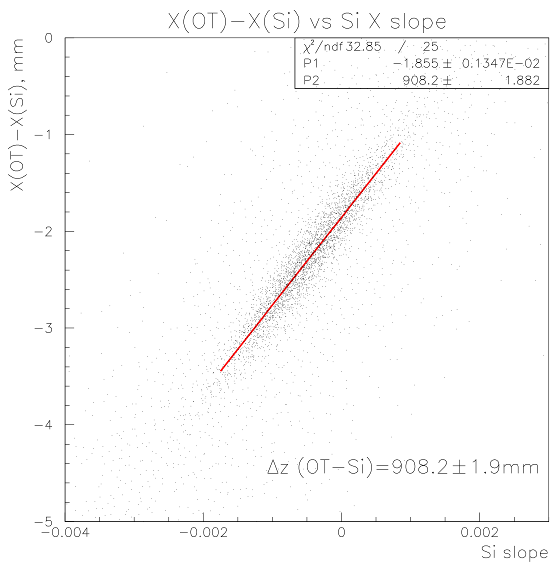

Figure 4: *Measurement of the z position of the first OT plane (1580 V). with respect to the first Si plane. Additionally this shows that the OT and Si tracking are consistent with each other.*

The parameters of the tracks measured with the Si are determined at the z coordinate (along the beam direction) of the first Si plane. The track reconstruction in OT gives parameters determined at the z position of plane 1. The measurement of the position of the first OT module with respect to the Si telescope was performed by comparing the track parameters as reconstructed in Si and OT in runs where both measurements are present and all the OT planes are at nominal voltage and threshold. The z position of the first OT plane was determined from a linear fit of the dependence of the difference between x coordinates, measured in OT (at z of OT plane 1) and Si (at z of Si plane 1), as a function of the track slope as measured with the Si.

The scatter plot of the correlation between these two values and the result of the linear fit are shown in Fig.4, indicating that the OT track reconstruction is consistent with the track reconstruction from the Si telescope.

OT mod	Plane	Δz(mm) plane-Si1	Δx(mm) run<1330	Δx(mm) run>1331
1	1	0.0	0	0
1	2	5.5	-2.504	-2.499
2	3	58.0	-1.272	-1.695
2	4	63.5	1.382	1.042
3	5	193.0	-1.749	-1.406
3	6	198.5	-4.023	-3.846
4	7	254.0	0.582	0.323
4	8	259.5	-1.945	-2.356

Table 1: *The relative positions of the OT planes used in the analysis. The* Δz *distances between the OT modules are obtained from ruler measurements. The absolute* z *position of the whole OT system is taken from Fig.4. The shifts in* x *are obtained from the analysis.*

3.3 Study of OT position measurement performance

In both approaches, including the Si telescope and OT standalone, the coordinate resolution was determined as the width of the distribution of the track residuals.

In the OT standalone analysis the resolution values obtained from the track residuals are biased, because of the finite precision of the track parameters themselves: for the hits excluded from the track reconstruction the resolution given by residuals is overestimated, while for those included into the track it is underestimated. In order to obtain an unbiased estimate of resolution, we applied a correction based on covariance matrix of track parameters [2]. All values of the resolution determined with OT standalone analysis are obtained with this correction, if not explicitly stated otherwise.

In the studies including the Si telescope the $t(r)$ relations necessary to evaluate the OT coordinate resolution were determined from correlation between the predicted track distance to a wire, by slicing the distribution in bins of the predicted x position. In the OT standalone analysis the $t(r)$ relation follows from an iterative procedure described in [2]. The results of both procedures were found to be consistent.

Fig.5*a,b* shows the correlation between the OT drift time and the track distance to wire as estimated with the Si (*a*) and with the 7 other OT planes (*b*), respectively. In order to evaluate the OT coordinate resolution, the inverse $t(r)$ relation was used to convert the drift time into coordinate. Subsequently the track residuals were calculated as a difference between the track prediction and the coordinate as obtained from the drift time. The value of the resolution was determined as a variance of a gaussian fit of the residual distribution. In Fig.5*c, d* the corresponding distributions of the track residuals together with the superimposed fitting curves are shown for both procedures. Note that the residuals shown for the OT standalone analysis (Fig.5*d*) were not corrected for the finite track reconstruction resolution, hence the width of its gaussian fit is an *upper limit* for the resolution. The residual distribution when using the track predictions from the Si is broader, which is caused by multiple scattering.

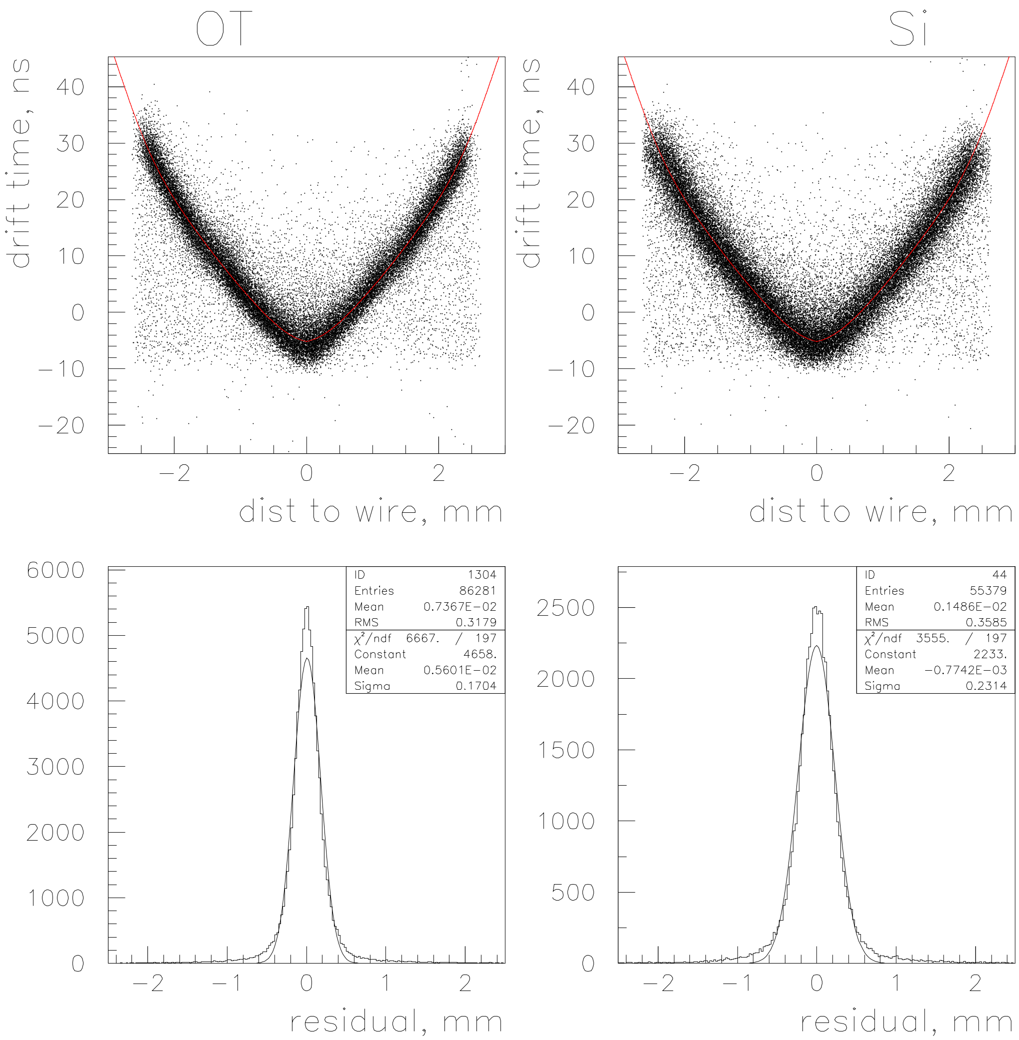

Figure 5: *Study of track reconstruction performance, plane 3. The correlation between OT drift time (at 1580 V, 700 mV) and track distance to wire determined with Si (b) and 7 other OT planes (a); the superimposed curve is fitted rt-relation. Corresponding distributions of track residuals (c), (d). The effect of multiple scattering leads to broader residuals distribution in case of using track predictions from Si.*

3.4 Efficiency

The straw efficiency profile, *ie* the dependence of the straw efficiency on the distance between track and wire, is shown in Fig.6. The track parameters were estimated using the other 7 planes of OT. The small but nonzero efficiency outside the straw boundary is caused by effects of electronics noise, crosstalk and also from finite accuracy of track parameters evaluation.

The average efficiency of an OT plane was defined as

$$\epsilon = \frac{N_{hit}}{N_{track}} \cdot g \ , \tag{1}$$

where N_{track} is number of events under study, N_{hit} is number of events where a hit occured in either the straw where the track points to or one of the two straws immediately neighbouring to it, g is the geometrical factor which is equal to the ratio of the wire pitch to the straw inner diameter: $g = \frac{5.25\text{mm}}{4.90\text{mm}} \approx 1.071$. This definition of the efficency is used in the final results in Section 5.

In other words, this efficiency corresponds to the single-cell efficiency, and the largest deviations from 100% can be attributed to the drop in efficiency at the edges of the straw, The efficiency is about 99% at the centre of the cell.

Note that there is no correction applied for noise contributions to the efficiency. This correction is very small for high true single cell efficieny, ϵ', and small values of the noise, n:

$$\epsilon = \epsilon' + (1 - \epsilon')n.$$

For an efficiency of 95% and a noise rate of 0.1%, the efficiency would be overestimated by 0.005%.

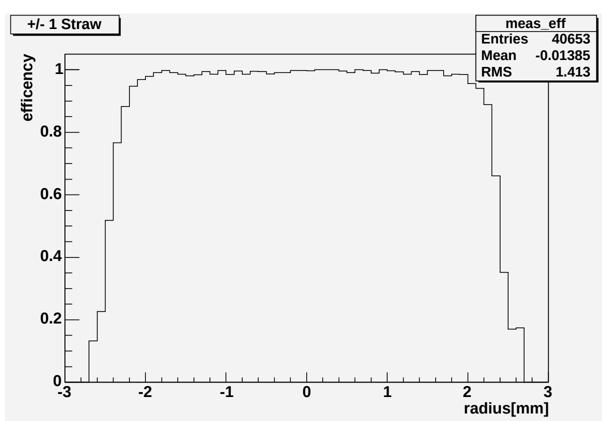

Figure 6: *The straw efficiency profile is shown.*

3.5 Cross Talk

The cross talk is defined as the probability that either of the two neighbouring straws produces a hit if the straw produces a hit caused by the particle track.

The hit distribution for plane 3 is shown in Fig.7*a* for those events in which the track points to the wire 41 and there is a hit in this wire which is compatible with the track. The high voltage at plane 3 in this run was 1700 V. The hits in the neighbouring channels (40 and 42) are mostly caused by crosstalk.

The time difference between crosstalk hits in channels 40 and 42 and track hit in channel 41 is shown in Fig.7*b*, showing a causal correlation between the hit, and the neigbouring cross talk hit. The majority of hits in these channels occur in about the same time after the hit in channel 41, indicating that it is indeed crosstalk.

The distribution of time difference for other (non-neighbouring) channels is shown in Fig7*c*. One can see that most of these hits come at random time, showing that these hits are mostly noise hits.

The strength of crosstalk is one of the important parameters for the choise of the working point of the OT detector. The average probability to have a crosstalk hit in neighbouring channels is used as an appropriate measure. The correction for noise was done by subtracting the probability to have a hit in non-neighbouring channels.

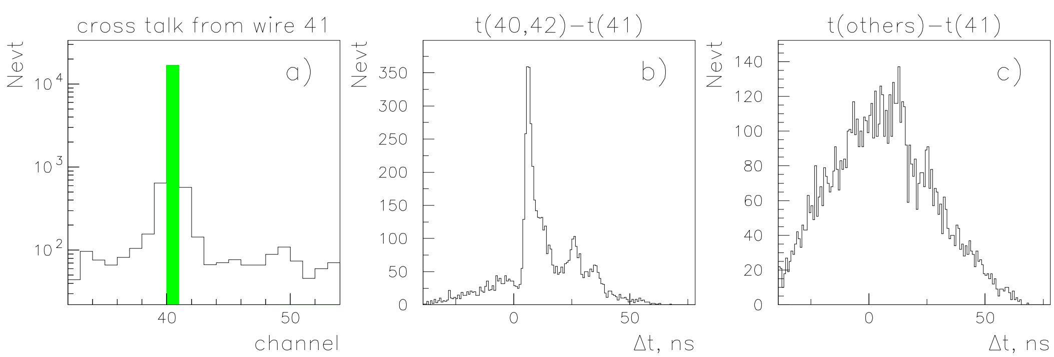

Figure 7: *The straw hit map (a) is shown for those tracks that point to straw 41. There is a significant probability for the neighboring straws to be hit, at this run taken at 1700 V. The time difference distributions for neighbouring (b) and non-neighbouring (c) channels show that hits in neghbouring channels mainly come from crosstalk, while in other channels they are mostly noise.*

4 Available data sets

The properties of OT modules were studied with respect to variation of high voltage and ASDBLR threshold voltage around their nominal values, which were U_{HV}=1580 V and U_{thr}=700 mV.

Also, the beam energy has varied to estimate the contribution to the resolution form the multiple scattering. The scintillator between the silicon station and the OT has been removed at run 1278.

The OT modules were installed on the vertically moveable support, so the position of the beam spot along the wire could be varied within 45 cm. Two vertical positions of the chambers were used, one with beam spot near the ends of the wires and another at 45 cm from the ends. In what follows these positions will be referred to as “high” and “low”, respectively. The OT modules 1, 3 and 4 were installed with frontend electronics box up, and module 2 with electronics box down. Therefore the chamber 2 was studied at distance y=0 and 45 cm from preamplifiers, while other chambers at y=225 and 180 cm, respectively, in “high” and “low” positions.

The following data sets were taken:

Runs	OT vert.pos.	Threshold (mV)	HV (V)	Si	Sci	E_{beam} (GeV)
1206–1243	high	575–900	1600	yes	yes	6
1312	high	700	1600	yes	no	6
1320–1330	high	700	1200–1700	no	no	6
1331–1341	low	700	1200–1700	no	no	6
1342–1351	low	800	1200–1700	no	no	6
1362–1368	low	650–800	1580	no	no	6
1370	low	700	1580	yes	no	6

Table 2: *Available data sets. Note that the HV and the amplifier threshold of the 1^{st} and 4^{th} module is always at 1580 V and 700 mV, respectively.*

5 Results

The resolution, efficiency and cross talk are presented as a function of HV in Fig.10. This analysis has been performed with the OT only. The increase of the cross talk with the beam at 45 cm distance from the amplifier is not understood. This is **not** observed with the beam close to the amplifier, for which a larger signal is expected. It is also **not** observed for the other module, were the beam is far (200 cm and 245 cm) from the amplifier. This rise in the cross talk however is observed in **both** planes of the module.

The noise frequency as a function of the amplifier threshold is shown in Figs.8-9: a noise rate of 40 kHz per wire corresponds to an occupancy of 0.3%.

To illustrate the performance of the OT and its electronics, the key performance numbers are given for an example setting at HV=1550 V and an amplifier threshold at 800 mV:

HV	Thr		Eff	Res	Cross talk	Noise	Gain
1550 V	800 mV	4.0 fC	95.6%	198 μm	2.12 %	900 Hz/wire	55000

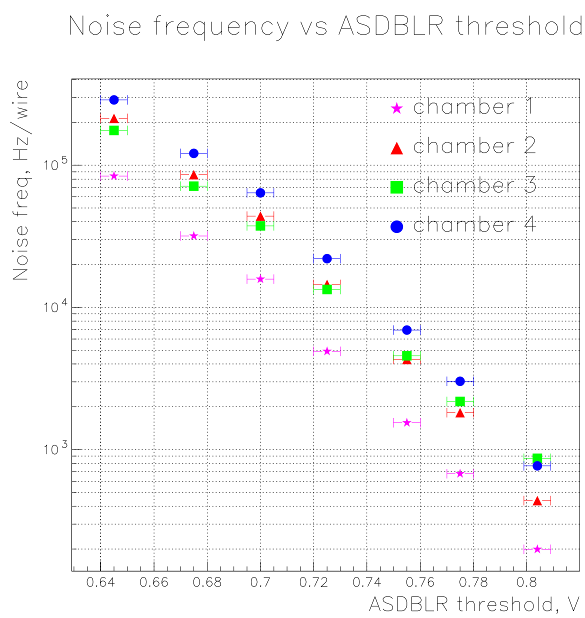

Figure 8: *The noise expressed in Hz/wire for the 4 modules. The first module shows an unexplained lower noise rate. The 1st module is different in such respect that the trigger signal from the scintillator counter is fed into the front end box of this module.*

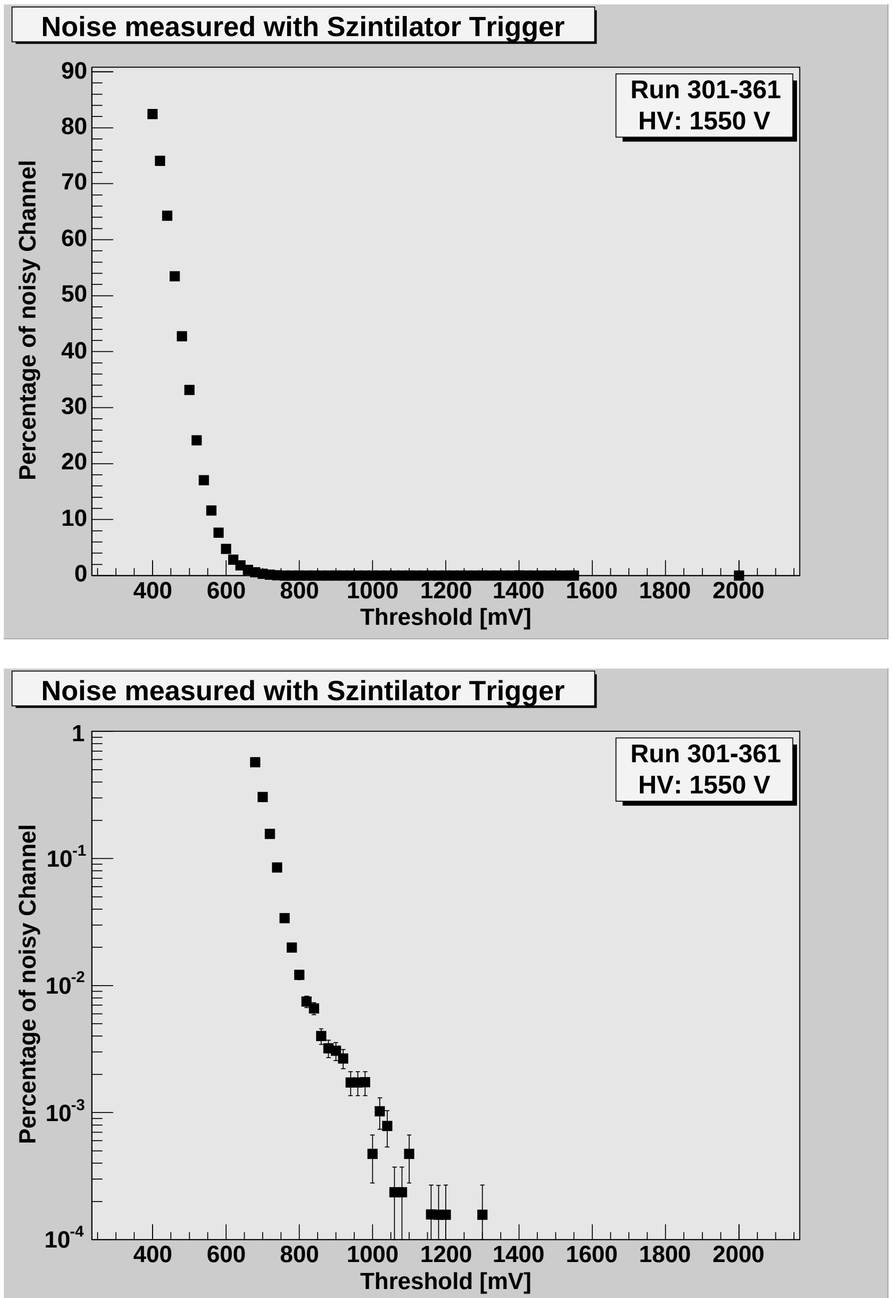

Figure 9: *The noise expressed as a probability to have a noise hit for module 1 (%). Noise values in the range from 400 mV to 1200 mV are shown. The difference between the upper and lower plots is the linear and logarithmic scale, respectively.*

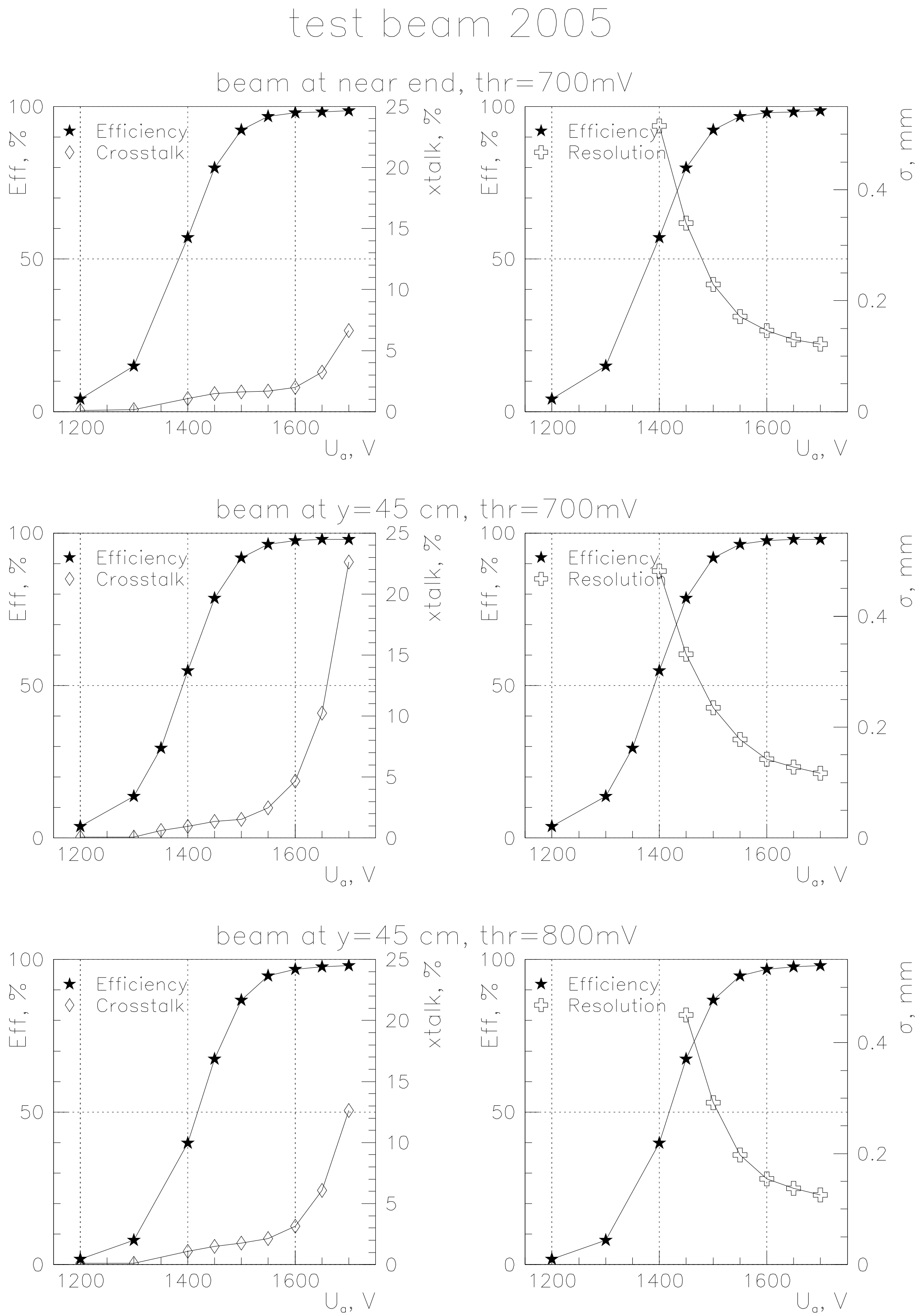

Figure 10: *The efficiency (as defined in Eq.(1)), resolution and cross talk of the OT plane 3 as a function of HV. Upper row: beam spot at the near (amplifier) end of the chamber,* U_{THR}*=700 mV. Middle row: beam spot at the distance of 45 cm from the amplifiers,* U_{THR}*=700 mV. Lower row: beam spot at 45 cm,* U_{THR}*=700 mV.*

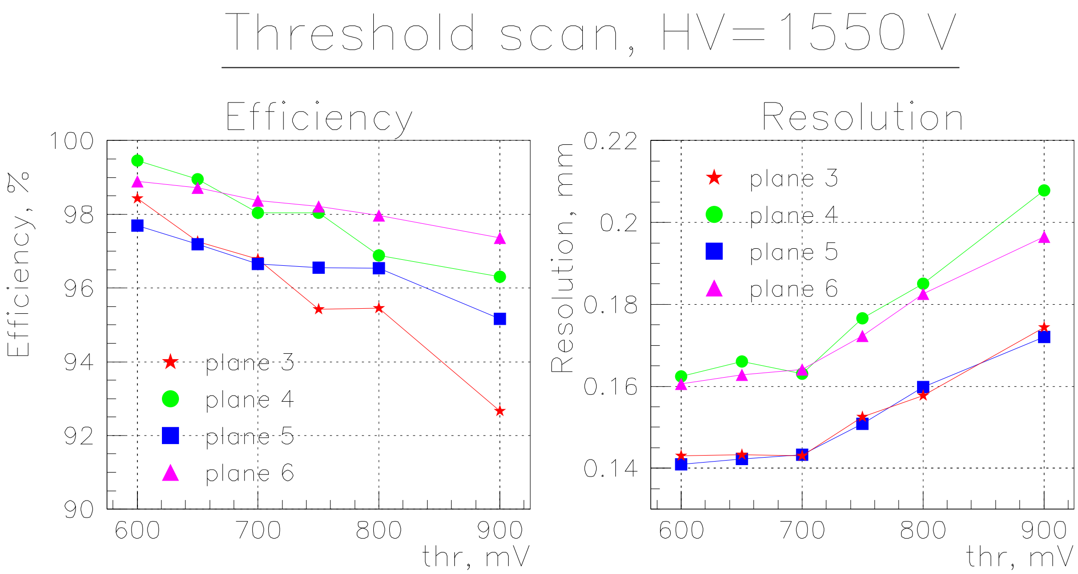

Figure 11: *The efficiency and resolution are plotted as a function of the threshold. The HV was set at 1550 V. Note that the beam is close to the front end electronics for lane 3 and plane 4 in module 2.*

References

[1] The LHCb Collaboration, P.R.Barbosa *et al.*,*Outer Tracker Techical Design Report*, CERN/LHCC 2001-024, Sept. 2001.

[2] W. Hulsbergen et al, *Calibration of HERA-B Outer Tracker Chambers in a Cosmic Ray Setup at NIKHEF*, HERA-B 00-014, Jan. 31, 2000. `http://www.nikhef.nl/pub/experiments/bfys/lhcb/outerTracker/Documents/Notes/herab-00-014.ps.gz`